Robust Cooperative Communication Optimization for Multi-UAV-Aided Vehicular Networks

Songge Zhang, Jianshan Zhou, Daxin Tian, *Senior Member, IEEE,* Zhengguo Sheng, *Senior Member, IEEE,* Xuting Duan, and Victor C. M. Leung, *Fellow, IEEE*

***Abstract*—Aerial-ground cooperative vehicular networks are envisioned as a novel paradigm in B5G/6G visions. In this letter, the challenge of optimizing the global energy-efficiency (EE) of multi-UAV-aided vehicular networks in the presence of uncertain air-to-ground (A2G) channels is addressed. Specifically, we propose a maximin paradigm to characterize the system, which aims to maximize its global EE meanwhile satisfying Quality-of-Service (QoS)-oriented data rate requirements in the worst-case situation. We theoretically derive a closed-form optimal solution for an embedded minimization subproblem under a parametric channel uncertainty set and thus develop a computationally tractable robust counterpart, which leads to a robust EE optimization design. Simulation results show that the proposed method significantly outperforms conventional EE schemes in terms of achieving higher global system performance and better robustness under random uncertain environments.**

***Index Terms*—Aerial-ground cooperative networks, unmanned aerial vehicles (UAVs), cooperative communication, energy efficiency, robust counterpart optimization.**

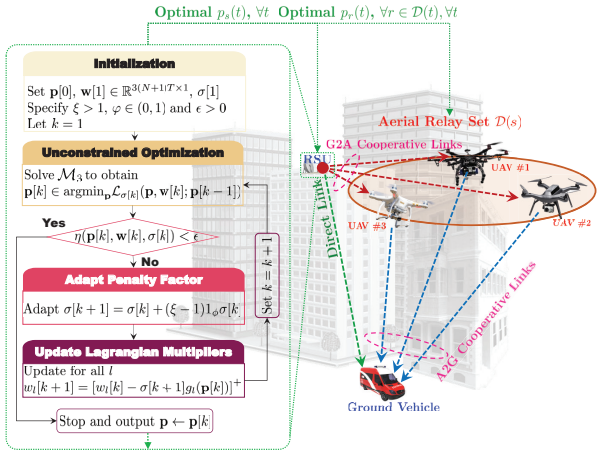

Fig. 1. A typical multi-UAV-aided vehicular network.

I. Introduction

In the visions of Beyond 5G (B5G) or even 6G systems, unmanned aerial vehicles (UAVs or drones) can act as flying relays to enhance the connectivity of ground vehicles by creating a cooperative communication network [1]. Since the onboard resources carried by the UAVs are quite limited, one key requirement is the energy-efficiency (EE) transmission optimization for the practical realization of a multi-UAV-aided vehicular network. However, due to inaccurate channel estimation, erroneous channel feedback or frequency offsets resulting from nodes' high mobility, there inherently exist disturbances and uncertainty in the channel state information (CSI) of air-to-ground (A2G) wireless links, which poses a great challenge and should be appropriately tackled in the practical system deployment.

Currently, many researchers are engaged in developing energy-efficiency UAV-aided communication and networking systems, such as cooperative UAV-assisted terrestrial cellular networks [2], UAV-assisted mobile edge computing systems [3], [4], space-air-ground integrated heterogeneous networks [5], etc. In these works, the energy-efficiency optimization of their targeted systems has been well addressed by exploiting either classical convex optimization approaches [2]–[4] or deep reinforcement learning-based approaches [5]. In other works such as [6], [7], UAV-enabled networks are optimized by jointly designing UAVs' trajectories and power control. Nevertheless, the aforementioned studies and most of those references therein are based on an implicit assumption that perfect CSI is available at both ends of an A2G link. Few works have taken into account channel disturbances and uncertainty in their system designs. Unfortunately, in reality, the aerial-ground cooperative system has to confront more general situations. Especially, the A2G channels inherently experience random disturbances and uncertainty. Hence, the channel imperfectness should be properly captured and handled in the system optimization, which essentially motivates our work.

In this letter, we address robust energy-efficiency optimization of multi-UAV-aided vehicular networks. Specifically, we explicitly characterize the imperfectness of the CSI on the A2G links by a parametric uncertainty set. We propose a maximin optimization model and then theoretically derive a closed-form solution for the nested minimization subproblem

This research was supported in part by the "Zhuoyue" Program of Beihang University (Postdoctoral Fellowship), the China Postdoctoral Science Foundation under Grant No. 2020M680299, the National Natural Science Foundation of China under Grant No. 61822101, Beijing Municipal Natural Science Foundation No. L191001 and 4181002, the Newton Advanced Fellowship under Grant No. 62061130221, the H2020-MSCA-RISE (101006411-SEEDS), and the Royal society Kan Tong Po International Fellowship. (S. Zhang and J. Zhou contributed equally to this work; Corresponding author: J. Zhou)

S. Zhang, J. Zhou, D. Tian and X. Duan are with Beijing Advanced Innovation Center for Big Data and Brain Computing, Beijing Key Laboratory for Cooperative Vehicle Infrastructure Systems & Safety Control, School of Transportation Science and Engineering, Beihang University, Beijing 100191, China (e-mail: zzuzsg@126.com, jianshanzhou@foxmail.com, dtian@buaa.edu.cn, duanxuting@buaa.edu.cn).

Z. Sheng is with Department of Engineering and Design, the University of Sussex, Richmond 3A09, UK (e-mail: z.sheng@sussex.ac.uk).

V. Leung is with Department of Electrical and Computer Engineering, The University of British Columbia, Vancouver, B.C., V6T 1Z4 Canada (e-mail: vleung@ieee.org).

under the channel uncertainty set. Based on this, we further develop a computationally tractable counterpart to maximize the worst-case EE performance. An novel iterative programming algorithm has also been proposed based on the theory of the augmented Lagrangian multipliers, which leads to a robust communication optimization design. The convergence and advantages of the proposed method in terms of both the global EE and robustness are also validated by extensive simulations. Our robust optimization design can cope with A2G channel uncertainty, relax the assumption on the perfectness of the A2G CSI that has been widely adopted in current literature, and thus facilitate the practical deployment of multi-UAV-aided vehicular communication systems.

II. System Model and Problem Formulation

As shown in Fig. 1, we consider a general multi-UAV-aided vehicular network, in which the physical-layer repetition-coded DF mechanism [1] can be used to realize the cooperative communications among ground networking vehicles and multiple flying UAVs as aerial relays. The ground source node, e.g., a Road-Side Unit (RSU), is denoted by s, while the set of the cooperative UAVs, also termed the aerial relay set, is denoted by $\mathcal{D}(s)$. Without loss of generality, let $|\mathcal{D}(s)| = N$, and the allowable maximum and minimum normalized transmission powers of a node $i \in \{s\} \cup \mathcal{D}(s)$ be $p_{i,\max}$ and $p_{i,\min}$, respectively. We consider a discrete-time system implementation and the index of a time slot with the duration τ is denoted by t. The total number of time slots is T, i.e., $t = 1, 2 \ldots, T$. The normalized transmission power of the source s at t is $p_s(t) \in [p_{s,\min}, p_{s,\max}]$ and that of a UAV $r \in \mathcal{D}(s)$ is $p_r(t) \in [p_{r,\min}, p_{r,\max}]$.

A. Mobility Model

Since the mobility of either the ground vehicle or the flying UAVs has a significant impact on the system performance, we would like to capture the mobility effect in the system modeling. To be specific, letting the 3-dimensional position, velocity and acceleration of a moving node $i \in \{s\} \cup \mathcal{D}(s)$ at t be $\mathbf{x}_i(t)$, $\mathbf{v}_i(t)$ and $\mathbf{a}_i(t)$, respectively, we characterize the kinematics of the node i by using the following time-discrete double integral model

$$\begin{cases} \mathbf{x}_i(t+1) = \mathbf{x}_i(t) + \tau \mathbf{v}_i(t) + \frac{\tau^2}{2}\mathbf{a}_i(t); \\ \mathbf{v}_i(t+1) = \mathbf{v}_i(t) + \tau \mathbf{a}_i(t). \end{cases} \tag{1}$$

Thus, the relative distance between any two moving nodes i' and i'' at t, $d_{i',i''}(t)$, can be estimated by

$$d_{i',i''}(t) = \|\mathbf{x}_{i'}(t) - \mathbf{x}_{i''}(t)\|_2, \ i', i'' \in \{s\} \cup \mathcal{D}(s). \tag{2}$$

B. Multi-Relay Cooperative Communication Model

With a given aerial relay set $\mathcal{D}(s)$, the maximum average mutual information of the source-destination link using the DF cooperative communication protocol [1] under the condition that each UAV in $\mathcal{D}(s)$ can successfully decode its received information from the source can be formulated as follows

$$I(t) = \frac{\tau B}{N+1} \log_2 \left(1 + \sum_{i \in \{s\} \cup \mathcal{D}(s)} \frac{p_i(t)|h_i(t)|^2}{d_i^{\alpha}(t)} \right), \tag{3}$$

where B is the totally available bandwidth; $d_i(t)$ is the relative distance between node i and the destination at t that can be calculated by (2); $h_i(t)$ is the coefficient capturing the channel fading characteristics over the link from node i to the destination at t; α is the path-loss factor.

Additionally, the condition for any UAV r successfully decoding the source's information is that the transmission data rate over the communication link from source s to r at t, denoted by $R_r(t)$, should not be smaller than a minimum requirement, r_1, in order to establish the cooperative communication. To practically characterize such a condition, we adopt a soft constraint that the outage probability of the s-to-r communication link, $\text{Prob}\{R_r(t) < r_1\}$, should not exceed a given threshold β, i.e.,

$$\text{Prob}\{R_r(t) < r_1\} \leq \beta, \ r \in \mathcal{D}(s), \tag{4}$$

in which $R_r(t)$ is given as follows [1]

$$R_r(t) = \frac{\tau B}{N+1} \log_2 \left(1 + \frac{p_s(t)|g_{s,r}(t)|^2}{d_{s,r}^{\alpha}(t)} \right), \tag{5}$$

where $g_{s,r}(t)$ characterizes the channel fading of the the s-to-r communication link at t, and $d_{s,r}(t)$ denotes the relative distance between s and r at t.

C. Channel Randomness and Uncertainty Model

Two types of communication channel are identified in our considered scenario as shown in Fig. 1. Specifically, we consider the effect of the heavily built-up urban environment on signal propagation. According to the existing literature [8]–[11], the frequency non-selective Rayleigh block fading can well capture the channel characteristics of the ground-to-air (G2A) uplinks, since there are many objects in the urban area, such as high-rise buildings and trees, that can scatter the G2A radio signal before it arrives at the aerial relays. Thus, we are allowed to exploit the Rayleigh fading distribution to model the stochastic G2A channels. Such a consideration results in the situation that $|g_{s,r}(t)|^2 d_{s,r}^{-\alpha}(t)$ is exponentially distributed with the parameter $d_{s,r}^{\alpha}(t)$. Therefore, the outage probability of the s-to-r uplink can be rearranged as

$$\text{Prob}\{R_r(t) < r_1\} = 1 - \exp\left(-\frac{\left(2^{\frac{r_1(N+1)}{\tau B}} - 1\right)}{p_s(t) d_{s,r}^{-\alpha}(t)} \right), \ r \in \mathcal{D}(s). \tag{6}$$

However, for the case of A2G communications, the channel fading can be much more complicated, and thus the uncertainty and imperfectness of the A2G channels, i.e., $h_i(t)$, $i \in \{s\} \cup \mathcal{D}(s)$, has to be taken into account here. Without loss of generality, the channel fading coefficient $h_i(t)$ can be further modeled by the combination of its nominal deterministic estimation $\hat{h}_i(t)$ and an uncertain disturbance $\Delta h_i(t)$, i.e.,

$$h_i(t) = \hat{h}_i(t) + \Delta h_i(t), \ i \in \{s\} \cup \mathcal{D}(s). \tag{7}$$

For simplicity, we let the global channel uncertainty be

$$\Delta \mathbf{h}(t) \triangleq \text{col}\left\{ \Delta h_i(t), \ i \in \{s\} \cup \mathcal{D}(s) \right\}, \ \forall t, \tag{8}$$

and consider that the channel uncertainty is bounded within a norm ball $\mathcal{U}_\rho$ with a radius ρ as follows

$$\mathcal{U}_\rho \triangleq \left\{ \Delta\mathbf{h}(t) \in \mathbb{R}^{(N+1)\times 1} : \|\Delta\mathbf{h}(t)\|_2 \le \rho \right\}. \quad (9)$$

$\mathcal{U}_\rho$ is also termed a spherical uncertainty region, which has been widely adopted in the theory of robust optimization [12]. The radius ρ indicates the size of the channel uncertainty region, which implies the amount of the channel uncertainty. A larger value of ρ indicates higher uncertainty in the channels.

D. Maxmin Optimization Paradigm

With the goal of maximizing the overall energy efficiency of the network, we define the following system performance metric over T time slots

$$J = J\left(\mathbf{p}(1), \ldots, \mathbf{p}(T)\right) = \frac{\sum_{t=1}^{T} I(t)}{\sum_{t=1}^{T} \sum_{i\in\{s\}\cup\mathcal{D}(s)} p_i(t)}, \quad (10)$$

where the decision vector $\mathbf{p}(t)$ is the collection of the ground source's and the aerial relays' transmission powers at t, i.e., $\mathbf{p}(t) = \mathrm{col}\{p_i(t), i \in \{s\} \cup \mathcal{D}(s)\}$. The objective function J indeed represents the achievable transmission data rate per power consumption by the network system.

Besides, we also consider a lower bound on the cooperative transmission data rate $I(t)$, i.e., proposing the nonlinear constraint $I(t) \ge r_2$ where r_2 is a given minimum data rate requirement for guaranteeing the system QoS. Let $\mathbf{p}_{\min} = \mathrm{col}\{p_{i,\min}, i \in \{s\} \cup \mathcal{D}(s)\}$ and $\mathbf{p}_{\max} = \mathrm{col}\{p_{i,\max}, i \in \{s\} \cup \mathcal{D}(s)\}$. Due to the presence of the channel uncertainty $\Delta\mathbf{h}(t)$, $t = 1, \ldots, T$ in both the objective function and the nonlinear constraint, it is difficult and impractical to directly solve an EE optimal solution for the system. Instead, we turn to optimize the system performance J in the worst case of the A2G channels so as to provide a robust design, which leads to a maximin formulation as follows

$$\mathcal{M}_1: \max_{\mathbf{p}(t), t=1,\ldots,T} \min_{\Delta\mathbf{h}(t), t=1,\ldots,T} J\left(\mathbf{p}(1), \ldots, \mathbf{p}(T)\right) \quad s.t. \begin{cases} \mathrm{Prob}\{R_r(t) < r_1\} \le \beta,\ r \in \mathcal{D}(s); \\ I(t) \ge r_2,\ \Delta\mathbf{h}(t) \in \mathcal{U}_\rho; \\ \mathbf{p}(t) \in [\mathbf{p}_{\min}, \mathbf{p}_{\max}]; \\ t = 1, \ldots, T. \end{cases} \quad (11)$$

It can be found that another challenge arises from the nested minimization subproblem in the above maxmin model. The uncertain parameters $\{\Delta\mathbf{h}(t), \forall t\}$ are treated as the decisions that are highly coupled with the power controls $\{\mathbf{p}(t), \forall t\}$. In the following, we would like to propose a computationally tractable optimization method for $\mathcal{M}_1$.

III. Robust Counterpart Optimization

A. Robust Counterpart

Recalling that the channel uncertainty $\Delta\mathbf{h}(t)$ is involved in $I(t)$, we can formulate the lower bound of $I(t)$ over the channel uncertainty region $\mathcal{U}_\rho$ as

$$\theta(\mathbf{p}(t)) = \min_{\Delta\mathbf{h}(t)\in\mathcal{U}_\rho} \left\{ \frac{\tau B}{N+1} \log_2 \left(1 + \sum_{i\in\{s\}\cup\mathcal{D}(s)} \frac{p_i(t) \left| \hat{h}_i(t) + \Delta h_i(t) \right|^2}{d_i^\alpha(t)} \right) \right\} \quad (12)$$

and see $I(t) \ge \theta(\mathbf{p}(t))$ for $t = 1, \ldots, T$. With $\theta(\mathbf{p}(t))$, we further present the robust counterpart associated with $\mathcal{M}_1$

$$\mathcal{M}_2: \max_{\mathbf{p}(t), t=1,\ldots,T} \frac{\sum_{t=1}^{T} \theta(\mathbf{p}(t))}{\sum_{t=1}^{T} \sum_{i\in\{s\}\cup\mathcal{D}(s)} p_i(t)} \quad s.t. \begin{cases} \mathrm{Prob}\{R_r(t) < r_1\} \le \beta,\ r \in \mathcal{D}(s); \\ \theta(\mathbf{p}(t)) \ge r_2; \\ \mathbf{p}(t) \in [\mathbf{p}_{\min}, \mathbf{p}_{\max}]; \\ t = 1, \ldots, T. \end{cases} \quad (13)$$

In fact, $\theta(\mathbf{p}(t))$ indicates the worst-cast transmission data rate by aerial-ground cooperative communications. $\mathcal{M}_2$ is a robust counterpart model for the worst-case optimization of the system. Now, the key point to effectively solve $\mathcal{M}_2$ lies in the calculation of $\theta(\mathbf{p}(t))$. Based on (12), we can further derive the following closed form:

Theorem 1: The feasible lower bound of the aerial-ground cooperative transmission data rate $I(t)$ is expressed as

$$\theta(\mathbf{p}(t)) = \max \left\{ r_2, \frac{\tau B}{N+1} \log_2 \left(1 + \sum_{i\in\{s\}\cup\mathcal{D}(s)} \frac{p_i(t) d_i^\alpha(t) \left(\lambda^* \hat{h}_i(t)\right)^2}{\left(\lambda^* d_i^\alpha(t) + p_i(t)\right)^2} \right) \right\} \quad (14)$$

where the parameter λ^* is given as

$$\lambda^* = \arg \left\{ \lambda \in \mathbb{R}_+ : \rho^2 = \sum_{i\in\{s\}\cup\mathcal{D}(s)} \left| \frac{p_i(t) d_i^{-\alpha}(t) \hat{h}_i(t)}{\lambda + p_i(t) d_i^{-\alpha}(t)} \right|^2 \right\}. \quad (15)$$

Proof: Theorem 1 results from the Karush-Kuhn-Tucker (KKT) conditions, the proof of which is provided in Appendix A that can be found in the online supplementary materials. ■

B. Robust Optimization Algorithm

As can be seen, the robust counterpart $\mathcal{M}_2$ based on Theorem 1 is computationally tractable, which can motivate a practical optimization design. Here, we consider to solve the robust counterpart model by iterative programming. For simplicity, we let $\mathbf{p} = \mathrm{col}\{\mathbf{p}(t), t = 1, \ldots, T\}$ and denote all the inequality constraints including the bound constraints by $g_l(\mathbf{p}) = \beta - \mathrm{Prob}\{R_r(t) < r_1\} \ge 0$ for $l = 1, \ldots, NT$, $g_l(\mathbf{p}) = \theta(\mathbf{p}(t)) - r_2 \ge 0$ for $l = 1 + NT, \ldots, (N+1)T$, $g_l(\mathbf{p}) = p_i(t) - p_{i,\min} \ge 0$ for $l = (N+1)T+1, \ldots, 2(N+1)T$ and $g_l(\mathbf{p}) = p_{i,\max} - p_i(t) \ge 0$ for $l = 2(N+1)T + 1, \ldots, 3(N+1)T$. Note that the total number of the inequality constraints is $3(N+1)T$. We further derive the following result for $\mathcal{M}_3$ based on the Lagrangian optimization theory:

Theorem 2: A local optimal point of the unconstrained optimization model $\mathcal{M}_3$ with a given sufficiently large positive real number $\sigma > 0$ is equivalent to that of $\mathcal{M}_2$

$$\mathcal{M}_3: \min_{\mathbf{p},\mathbf{w}} \mathcal{L}_\sigma(\mathbf{p}, \mathbf{w}), \quad (16)$$

where $\mathbf{w} = \mathrm{col}\{w_l\} \in \mathbb{R}^{3(N+1)T\times 1}$ is the column vector collecting Lagrangian multipliers and $\mathcal{L}_\sigma(\mathbf{p}, \mathbf{w})$ is the augmented Lagrangian function as follows

$$\mathcal{L}_\sigma(\mathbf{p}, \mathbf{w}) = V(\mathbf{p}) + \frac{1}{2\sigma} \sum_{l=1}^{3(N+1)T} \left\{ \left[w_l - \sigma g_l(\mathbf{p}) \right]^{+2} - w_l^2 \right\} \quad (17)$$

in which $[x]^+ = \max\{0, x\}$ and we let the inverse objective function of $\mathcal{M}_3$ be $V(\mathbf{p})$.

Proof: Theorem 2 follows the Lagrangian optimization technique. The proof is detailed in Appendix B, which can be found in the online supplementary materials. ■

Based on Theorem 2, we can devise an effective iterative programming algorithm to obtain the solution of $\mathcal{M}_2$, since there already exist many highly efficient numerical optimization algorithms for solving the unconstrained counterpart $\mathcal{M}_3$. Specifically, given the current feasible point $\mathbf{p}[k-1]$, the current Lagrangian multipliers $\mathbf{w}[k]$ and the current penalty factor $\sigma[k]$ at an algorithmic iteration k, the update formulations for obtaining new iterative points $\mathbf{p}[k]$, $\mathbf{w}[k+1]$ and $\sigma[k+1]$ can be established as follows

$$\begin{cases} \mathbf{p}[k] \in \operatorname{argmin}_{\mathbf{p}} \mathcal{L}_{\sigma[k]}(\mathbf{p}, \mathbf{w}[k]; \mathbf{p}[k-1]); \\ \sigma[k+1] = \sigma[k] + (\xi - 1) 1_{\phi} \sigma[k]; \\ w_l[k+1] = [w_l[k] - \sigma[k+1] g_l(\mathbf{p}[k])]^+, \forall l, \end{cases} \tag{18}$$

where the parameter $\xi > 1$ is the increment coefficient, 1_{ϕ} is an indicator that is equal to 1 only if $\phi > 0$, otherwise 0. ϕ is a condition function defined as follows

$$\phi = \frac{\eta(\mathbf{p}[k], \mathbf{w}[k], \sigma[k])}{\eta(\mathbf{p}[k-1], \mathbf{w}[k-1], \sigma[k-1])} - \varphi \tag{19}$$

where $\varphi \in (0, 1)$ is a threshold and $\eta(\mathbf{p}[k], \mathbf{w}[k], \sigma[k])$ is a 2-norm stopping criteria function

$$\eta(\mathbf{p}[k], \mathbf{w}[k], \sigma[k]) = \left\{ \sum_{l=1}^{3(N+1)T} \left[\min\left(g_l(\mathbf{p}[k]), \frac{w_l[k]}{\sigma[k]} \right) \right]^2 \right\}^{\frac{1}{2}}. \tag{20}$$

Based on (18), Fig. 1 also illustrates the implementation framework of our proposed iterative programming algorithm for the robust counter optimization. In Fig. 1, $\epsilon > 0$ is a sufficiently small threshold for stopping the iterations. The key step here is to solve an unconstrained subproblem $\mathcal{M}_3$, which can be efficiently achieved by using existing methods such as the well-known Newton's method or the conjugate gradient descent method. Let the upper bounds on the sequences $\{\sigma[k]\}$ and $\{\eta(\mathbf{p}[k], \mathbf{w}[k], \sigma[k])\}$ be σ_{upper} and η_{upper}, respectively, i.e., $\sigma[k] \leq \sigma_{\text{upper}}$ and $\eta(\mathbf{p}[k], \mathbf{w}[k], \sigma[k]) \leq \eta_{\text{upper}}$. According to the complexity theory of the augmented Lagrangian method [13], the worst-case complexity of the outer-loop algorithm shown in Fig. 1 can be evaluated in the order of

$$\mathcal{O}\left(N(\epsilon) \times \frac{\log\left(\sigma_{\text{upper}}/\sigma[0]\right)}{\log(\xi)} \times \frac{\log(\epsilon/\eta_{\text{upper}})}{\log(\varphi)} \right), \tag{21}$$

where $N(\epsilon)$ denotes the complexity for solving the unconstrained optimization $\mathcal{M}_3$ and can be in the order of $\mathcal{O}(\epsilon^{-\frac{3}{2}})$ when using the Newton's method [14].

IV. Performance Evaluation

A. Simulation Parameters

We evaluate the proposed robust optimization method via simulations, in which the total number of simulation time slots is $T = 100$ and each slot duration is $\Delta\tau = 0.1\,\text{s}$. A RSU as a source is located at $(0, 0, 0)\,\text{m}$, and a ground vehicle as a destination is initially located at $(100, 0, 0)\,\text{m}$. The vehicle is moving at an initial velocity of $25\,\text{m/s}$ with a constant acceleration of $1\,\text{m/s}^2$ in the positive longitudinal direction. A platoon of UAVs as a group of aerial relays with a fixed flight height of $50\,\text{m}$ are initially located above the RSU and are flying towards the ground vehicle. Their longitudinal velocity and the space headway are set to $40\,\text{m/s}$ and $10\,\text{m}$, respectively. Throughout the simulations, the upper and lower power bounds are set to $p_{i,\max} = 40\,\text{dBm}$ and $p_{i,\min} = -40\,\text{dBm}$ for all $i \in \{s\} \cup \mathcal{D}(s)$. Additionally, the other physical-layer communication parameters are set as in [15]: the total available bandwidth is $B = 10\,\text{MHz}$, the channel noise power over 10 MHz is $-95\,\text{dBm}$, the antenna gain at each receiver is $3\,\text{dB}$ along with a path loss of $47.86\,\text{dB}$ per meter, and the path loss exponent is $\alpha = 2.75$. The data rate thresholds are set to $r_1 = 1\,\text{Kbits}$ and $r_2 = 1.45\,\text{Mbits}$, respectively. The 2-norm bound on the uncertain channel disturbances is $\rho = 2 \times 10^{-3}$. $\epsilon = 1 \times 10^{-3}$, $\sigma = \varphi = 0.8$ and $\xi = 1.5$ are adopted for the algorithm implementation.

B. Convergence Analysis and Performance Comparison

Fig. 2(a) shows that the global convergence of our proposed method can be well guaranteed with different UAV numbers. Specifically, the worst-case global energy-efficiency (EE) performance can effectively converge by only 250 iterations even when the number of the aerial nodes is relatively large, i.e., $N = 10$. Moreover, the first-order measure in Fig. S.2 in Appendix D of the online supplementary materials also confirm the convergence. In Fig. 2(b), we compare our method (Robust-EEO) with different benchmark methods based on the stochastic power control (Stochastic-Power) and the maximum power control (Max-Power) in ideal situations without any uncertain channel disturbance. Our method achieves the highest EE performance, the average level of which is about $17.41\,\text{Mbit/s/W}$ and $17.47\,\text{Mbit/s/W}$ higher than that of the Stochastic-Power method and the Max-Power method, respectively. The main reason is that when the channel uncertainty has not been considered, our method boils down to the ideal EE maximization, which can optimize the aerial-ground cooperative system performance as much as possible.

Moreover, we compare our proposed method with the conventional EE optimization (Conventional EEO) based on the widely-adopted sequential convex approximation approach in the presence of uncertain channel disturbances. Fig. 2(c) illustrates the worst-case throughput of the aerial-ground nodes under different N. As can be seen, the throughput performance of our proposed method is about 2 times higher than that of the Conventional EEO with $N = 2, 4$. Even with larger UAV numbers, e.g., $N = 6, 8, 10$, our method can also outperform the Conventional EEO by improving 38.23% throughput on average. This is because the conventional approach fails in dealing with the channel uncertainty. In addition, we carry out extensive Monte Carlo simulations, with 5000 replications per experimental condition, to examine the robustness of both the methods, in which the channel uncertainty $\Delta\mathbf{h}(t)$ is randomly generated by following the normal distribution for all t. Fig. 3 demonstrates the frequency distributions of the network data

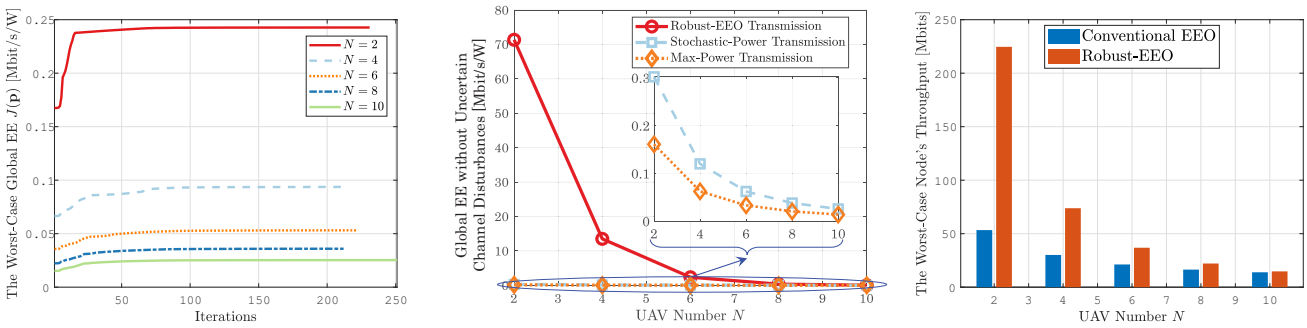

(a) Global Convergence with Different UAV numbers

(b) Global EE Performance without Uncertain Channel Disturbances

(c) Worst-Case Performance with Uncertain Channel Disturbances

Fig. 2. Simulation results.

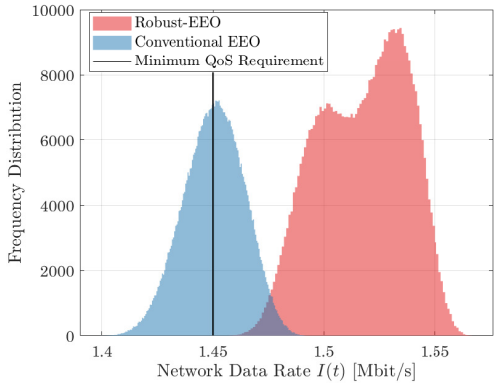

Fig. 3. System Robustness against Uncertain Channel Disturbances.

rate $I(t)$ achieved by these two methods. It is observed that the conventional EEO can satisfy the minimum QoS requirement with only about 50% probability, while our method can always guarantee QoS regardless of random channel disturbances, i.e., the probability of the data rate constraint satisfaction is 100%.

V. Conclusion

In this letter, we have proposed a robust counterpart optimization method to achieve the global energy-efficiency maximization of multi-UAV-aided networks with uncertain aerial-ground cooperative communication channels. Importantly, we have proposed a maximin model and theoretically derived a closed-form solution for its embedded subproblem, which enables a computationally tractable robust design. We propose a novel algorithm that re-formulates the constrained robust optimization into an unconstrained iterative programming paradigm and thus reduces the implementation complexity. Simulation results have verified the convergence of our method and its superior performance over several classical schemes in terms of global energy efficiency and robustness against random channel disturbances and uncertainty.

References

[1] J. N. Laneman and G. W. Wornell, "Distributed space-time-coded protocols for exploiting cooperative diversity in wireless networks," *IEEE Transactions on Information Theory*, vol. 49, no. 10, pp. 2415–2425, Oct 2003.

[2] H. Wu, X. Tao, N. Zhang, and X. Shen, "Cooperative uav cluster-assisted terrestrial cellular networks for ubiquitous coverage," *IEEE Journal on Selected Areas in Communications*, vol. 36, no. 9, pp. 2045–2058, Sep. 2018.

[3] M. Li, N. Cheng, J. Gao, Y. Wang, L. Zhao, and X. Shen, "Energy-efficient uav-assisted mobile edge computing: Resource allocation and trajectory optimization," *IEEE Transactions on Vehicular Technology*, vol. 69, no. 3, pp. 3424–3438, March 2020.

[4] X. Hu, K. Wong, K. Yang, and Z. Zheng, "Uav-assisted relaying and edge computing: Scheduling and trajectory optimization," *IEEE Transactions on Wireless Communications*, vol. 18, no. 10, pp. 4738–4752, Oct 2019.

[5] N. Cheng, F. Lyu, W. Quan, C. Zhou, H. He, W. Shi, and X. Shen, "Space/aerial-assisted computing offloading for iot applications: A learning-based approach," *IEEE Journal on Selected Areas in Communications*, vol. 37, no. 5, pp. 1117–1129, May 2019.

[6] S. Fang, G. Chen, and Y. Li, "Joint optimization for secure intelligent reflecting surface assisted uav networks," *IEEE Wireless Communications Letters*, pp. 1–1, 2020.

[7] Y. Wu, W. Yang, X. Guan, and Q. Wu, "Energy-efficient trajectory design for uav-enabled communication under malicious jamming," *IEEE Wireless Communications Letters*, pp. 1–1, 2020.

[8] I. Y. Abualhaol and M. M. Matalgah, "Performance analysis of cooperative multi-carrier relay-based uav networks over generalized fading channels," *International Journal of Communication Systems*, vol. 24, no. 8, pp. 1049–1064, 2011. [Online]. Available: https://onlinelibrary.wiley.com/doi/abs/10.1002/dac.1212

[9] M. Simunek, F. P. Fontán, and P. Pechac, "The uav low elevation propagation channel in urban areas: Statistical analysis and time-series generator," *IEEE Transactions on Antennas and Propagation*, vol. 61, no. 7, pp. 3850–3858, July 2013.

[10] F. Jiang and A. L. Swindlehurst, "Optimization of uav heading for the ground-to-air uplink," *IEEE Journal on Selected Areas in Communications*, vol. 30, no. 5, pp. 993–1005, June 2012.

[11] W. Khawaja, I. Guvenc, D. W. Matolak, U. Fiebig, and N. Schneckenburger, "A survey of air-to-ground propagation channel modeling for unmanned aerial vehicles," *IEEE Communications Surveys Tutorials*, vol. 21, no. 3, pp. 2361–2391, thirdquarter 2019.

[12] A. Ben-Tal, L. E. Ghaoui, and A. Nemirovski, *Robust Optimization*, ser. Princeton Series in Applied Mathematics. Princeton University Press, 2009, vol. 28. [Online]. Available: https://doi.org/10.1515/9781400831050

[13] E. G. Birgin and J. M. Martínez, "Complexity and performance of an augmented lagrangian algorithm," *Optimization Methods and Software*, vol. 35, no. 5, pp. 885–920, 2020. [Online]. Available: https://doi.org/10.1080/10556788.2020.1746962

[14] C. Cartis, N. I. M. Gould, and P. L. Toint, "On the complexity of steepest descent, newton's and regularized newton's methods for nonconvex unconstrained optimization problems," *SIAM Journal on Optimization*, vol. 20, no. 6, pp. 2833–2852, 2010. [Online]. Available: https://doi.org/10.1137/090774100

[15] A. Bazzi, B. M. Masini, A. Zanella, and I. Thibault, "On the performance of ieee 802.11p and lte-v2v for the cooperative awareness of connected vehicles," *IEEE Transactions on Vehicular Technology*, vol. 66, no. 11, pp. 10 419–10 432, Nov 2017.

Supplementary Materials for Robust Cooperative Communication Optimization for Multi-UAV-Aided Vehicular Networks

Songge Zhang, Jianshan Zhou, Daxin Tian, *Senior Member, IEEE,* Zhengguo Sheng, *Senior Member, IEEE,* Xuting Duan, and Victor C. M. Leung, *Fellow, IEEE*

Appendix A
Proof of Theorem 1

Recalling (12) and the constraint $\theta(\mathbf{p}(t)) \geq r_2$, we can propose an equivalent subproblem as

$$\min_{\Delta\mathbf{h}(t)} f(\Delta\mathbf{h}(t)) = \sum_{i\in\{s\}\cup\mathcal{D}(s)} \frac{p_i(t)\left|\hat{h}_i(t)+\Delta h_i(t)\right|^2}{d_i^{\alpha}(t)}$$
$$s.t. \begin{cases} \sum\limits_{i\in\{s\}\cup\mathcal{D}(s)} \dfrac{p_i(t)\left|\hat{h}_i(t)+\Delta h_i(t)\right|^2}{d_i^{\alpha}(t)} \geq C; \\ \sum\limits_{i\in\{s\}\cup\mathcal{D}(s)} |\Delta h_i(t)|^2 \leq \rho^2. \end{cases} \tag{S.1}$$

where $C = 2^{\frac{r_2(N+1)}{\tau B}} - 1$. The Lagrangian function of (S.1) is then expressed as follows

$$\mathcal{L}(\Delta\mathbf{h}(t),\lambda,\gamma) = (1-\gamma)\sum_{i\in\{s\}\cup\mathcal{D}(s)} \frac{p_i(t)\left|\hat{h}_i(t)+\Delta h_i(t)\right|^2}{d_i^{\alpha}(t)} + \gamma C - \lambda\left(\rho^2 - \sum_{i\in\{s\}\cup\mathcal{D}(s)} |\Delta h_i(t)|^2\right) \tag{S.2}$$

where λ and γ are two nonnegative Lagrangian multipliers.

Based on the Karush-Kuhn-Tucker (KKT) conditions, the optimum point of (S.1) and the optimal Lagrangian multipliers, denoted by $\Delta\mathbf{h}^*(t)$, λ^* and γ^*, respectively, must satisfy

$$\begin{cases} \nabla_{\Delta\mathbf{h}}\mathcal{L}(\Delta\mathbf{h}^*(t),\lambda^*,\gamma^*) = \mathbf{0}, \gamma^* \geq 0, \lambda^* \geq 0; \\ \gamma^*\left(\sum\limits_{i\in\{s\}\cup\mathcal{D}(s)} \dfrac{p_i(t)\left|\hat{h}_i(t)+\Delta h_i^*(t)\right|^2}{d_i^{\alpha}(t)} - C\right) = 0; \\ \lambda^*\left(\rho^2 - \sum\limits_{i\in\{s\}\cup\mathcal{D}(s)} |\Delta h_i^*(t)|^2\right) = 0; \end{cases} \tag{S.3}$$

and the constraints of (S.1). Next, we can solve (S.3) in the following two cases:

i) If $\sum_{i\in\{s\}\cup\mathcal{D}(s)} |\Delta h_i^*(t)|^2 < \rho^2$, we can have $\lambda^* = 0$. The gradient condition and the second complementary slackness condition in (S.3) further lead to $\gamma^* = 1$ and $\sum_{i\in\{s\}\cup\mathcal{D}(s)} p_i(t)\left|\hat{h}_i(t)+\Delta h_i^*(t)\right|^2 d_i^{-\alpha}(t) = C$. This result indicates $\theta(\mathbf{p}(t)) = r_2$.

ii) If $\sum_{i\in\{s\}\cup\mathcal{D}(s)} |\Delta h_i^*(t)|^2 = \rho^2$, we can derive the nonzero Lagrangian multiplier $\lambda^* > 0$ as given by (15). Using the gradient condition and the second complementary slackness condition in (S.3), we can further solve

$$\Delta h_i^*(t) = -\frac{p_i(t)\hat{h}_i(t)d_i^{-\alpha}(t)}{\lambda^* + p_i(t)d_i^{-\alpha}(t)}, i \in \{s\}\cup\mathcal{D}(s) \tag{S.4}$$

and $\gamma^* = 0$. Substituting (S.4) into the objective function of (S.1) can lead to

$$\theta(\mathbf{p}(t)) = \frac{\tau B}{N+1}\log_2\left(1 + \sum_{i\in\{s\}\cup\mathcal{D}(s)} \frac{p_i(t)d_i^{\alpha}(t)\left(\lambda^*\hat{h}_i(t)\right)^2}{\left(\lambda^* d_i^{\alpha}(t) + p_i(t)\right)^2}\right). \tag{S.5}$$

Combining both results in the above two cases can prove the theorem.

Appendix B
Proof of Theorem 2

By introducing auxiliary variables $\mathbf{q} = \mathrm{col}\{q_l \in \mathbb{R}, l = 1,\ldots,3(N+1)T\}$, we can convert $\mathcal{M}_2$ into another equivalent constrained optimization with a set of equality constraints

$$\min_{\mathbf{p},\mathbf{q}} V(\mathbf{p}) \quad s.t.\ g_l(\mathbf{p}) - q_l^2 = 0, l = 1,\ldots,3(N+1)T. \tag{S.6}$$

For the above problem, the augmented Lagrangian function is

$$\mathcal{L}_{\sigma}(\mathbf{p},\mathbf{q},\mathbf{w}) = V(\mathbf{p}) - \sum_{l=1}^{3(N+1)T} w_l\left(g_l(\mathbf{p}) - q_l^2\right) + \frac{\sigma}{2}\sum_{l=1}^{3(N+1)T}\left[g_l(\mathbf{p}) - q_l^2\right]^2. \tag{S.7}$$

That is, solving $\mathcal{M}_2$ is equivalent to solve $\min \mathcal{L}_{\sigma}(\mathbf{p},\mathbf{q},\mathbf{w})$ with respect to $\mathbf{p}$, $\mathbf{q}$ and $\mathbf{w}$.

According to the KKT conditions, we can have the gradient results with respect to the auxiliary variables $\mathbf{q}$, i.e., $\nabla_{\mathbf{q}}\mathcal{L}_{\sigma}(\mathbf{p},\mathbf{q},\mathbf{w}) = \mathbf{0}$, which further lead to

$$q_l\left[\sigma q_l^2 - (\sigma g_l(\mathbf{p}) - w_l)\right] = 0,\ l = 1,\ldots,3(N+1)T. \tag{S.8}$$

Accordingly, if $\sigma g_l(\mathbf{p}) - w_l \geq 0$ then we have

$$q_l^2 = \frac{1}{\sigma}\left(\sigma g_l(\mathbf{p}) - w_l\right),\ l = 1,\ldots,3(N+1)T. \tag{S.9}$$

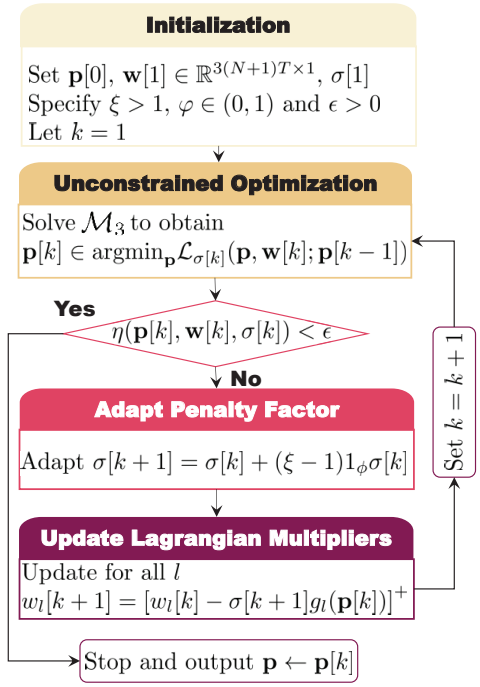

Fig. S.1. The implementation framework of the proposed iterative programming algorithm.

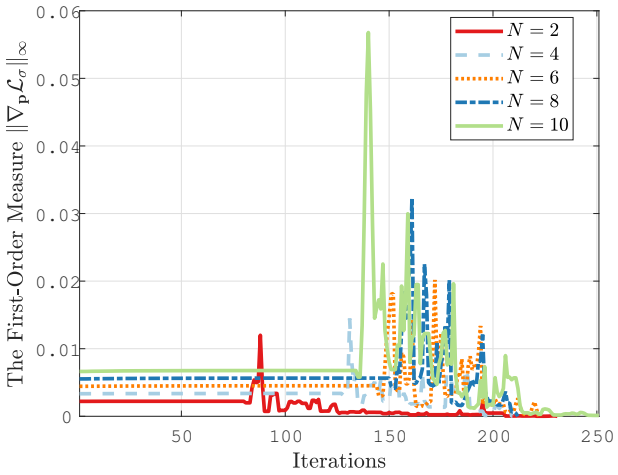

Fig. S.2. The First-Order Measure Variation with Different UAV numbers.

Otherwise, we can see $\sigma q_l^2 - (\sigma g_l(\mathbf{p}) - w_l) > 0$, which implies $q_l^2 = 0$. Combining both the results above can lead to

$$q_l^2 = \frac{1}{\sigma}\max\left\{\sigma g_l(\mathbf{p}) - w_l, 0\right\},\ l = 1, \ldots, 3(N+1)T. \tag{S.10}$$

Substituting (S.10) into (S.7) can prove the theorem.

Appendix C
The Algorithm Implementation Framework

In Fig. S.1, we illustrate the implementation framework of the proposed iterative programming algorithm. As can be seen, the proposed method can be effectively realized in practical application scenarios, since it does solve a series of unconstrained subproblems $\mathcal{M}_3$ instead of directly handling the complicated constrained optimization model $\mathcal{M}_2$.

Appendix D
The First-Order Measure on Convergence

We also supplement additional numerical results to validate the convergence of the proposed algorithm as in Fig. S.2. The figure shows the first-order measure variation on the augmented Lagrangian function $\mathcal{L}_{\sigma}$ under different numbers of UAVs N. It can be found that the first-order measure, $\|\nabla_{\mathbf{p}}\mathcal{L}_{\sigma}\|_{\infty}$, can approximately converge to 0 under different N, which indicates that the locally optimal robust solution has been achieved by our algorithm.